

# 10

## Non-WIMP Candidates<sup>†</sup>

Jonathan L. Feng

*Department of Physics and Astronomy, University of California, Irvine, CA 92697, USA*

### 10.1 Motivations

There are many non-WIMP dark matter candidates. Two prominent and highly motivated examples are axions and sterile neutrinos, which are reviewed in Chapters 11 and 12, respectively. In addition, there are candidates motivated by minimality, particles motivated by experimental anomalies, and exotic possibilities motivated primarily by the desire of their inventors to highlight how truly ignorant we are about the nature of dark matter.

In this brief Chapter, we focus on dark matter candidates that are not WIMPs, but which nevertheless share the most important virtues of WIMPs. As discussed in Chapters 7, 8, and 9, WIMPs have several nice properties:

- They exist in well-motivated particle theories.
- They are naturally produced with the correct thermal relic density (the “WIMP miracle”).
- They predict signals that may be seen in current and near future experiments.

The candidates we discuss also have all three of these properties. They fall naturally into two classes: superWIMP candidates, which inherit the correct relic density through decays, and WIMPless candidates, which have neither weak-scale masses nor weak interactions, but which nevertheless have the correct thermal relic density. These possibilities appear in the same particle physics frameworks as WIMPs, but they imply very different cosmological histories for our Universe, as well as qualitatively new dark matter signals for both astrophysical observatories and particle physics experiments.

<sup>†</sup>Published as Chapter 10, pp. 190-204, in *Particle Dark Matter: Observations, Models and Searches*, edited by Gianfranco Bertone (Cambridge University Press, 2010), available at <http://cambridge.org/us/catalogue/catalogue.asp?isbn=9780521763684>.

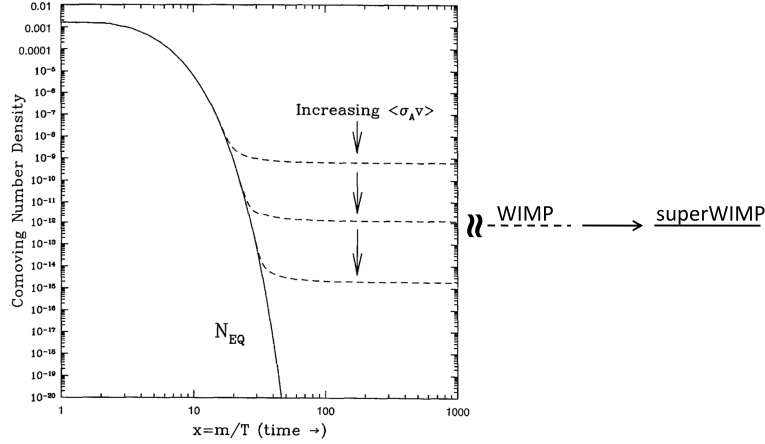


Fig. 10.1. In superWIMP scenarios, WIMPs freeze out as usual, but then decay to superWIMPs, superweakly-interacting massive particles that form dark matter.

## 10.2 SuperWIMP Dark Matter

### 10.2.1 Candidates and Relic Densities

In the superWIMP framework for dark matter, WIMPs freeze out as usual in the early Universe, but later decay to superWIMPs, superweakly-interacting massive particles that form the dark matter that exists today. Because superWIMPs are very weakly-interacting, they have no impact on WIMP freeze out in the early universe, and the WIMPs decouple, as usual, with a thermal relic density  $\Omega_{\text{WIMP}}$  that is naturally near the required density  $\Omega_{\text{DM}} \approx 0.23$ . Assuming that each WIMP decay produces one superWIMP, the relic density of superWIMPs is

$$\Omega_{\text{SWIMP}} = \frac{m_{\text{SWIMP}}}{m_{\text{WIMP}}} \Omega_{\text{WIMP}} . \quad (10.1)$$

SuperWIMPs therefore inherit their relic density from WIMPs, and for  $m_{\text{SWIMP}} \sim m_{\text{WIMP}}$ , they are also naturally produced in the desired amount to be much or all of dark matter. The evolution of number densities is shown in Fig. 10.1.

The superWIMP scenario is realized in many particle physics models. The prototypical example is gravitinos, which exist in all supersymmetric theories (44; 45; 43; 36; 17; 75; 48; 49; 46; 37; 71). In the simplest supersymmetric models, supersymmetry is transmitted to standard model superpartners through gravitational interactions, and supersymmetry is broken at a high

scale. The mass of the gravitino  $\tilde{G}$  is

$$m_{\tilde{G}} = \frac{F}{\sqrt{3}M_*} , \quad (10.2)$$

and the masses of standard model superpartners are

$$\tilde{m} \sim \frac{F}{M_*} , \quad (10.3)$$

where  $M_* = (8\pi G_N)^{-1/2} \simeq 2.4 \times 10^{18}$  GeV is the reduced Planck scale and  $F \sim (10^{11} \text{ GeV})^2$  is the supersymmetry-breaking scale squared. The precise ordering of masses depends on unknown, presumably  $\mathcal{O}(1)$ , constants in Eq. (10.3). It is, then, perfectly possible that the gravitino is the lightest supersymmetric particle (LSP) and a candidate for superWIMP dark matter. The role of the decaying WIMP is played by the next-to-lightest supersymmetric particle (NLSP), typically a slepton, sneutrino, or neutralino. As required, the gravitino couples very weakly, with interactions suppressed by  $M_*$ , and so it is irrelevant during the WIMP's thermal freeze out.

The gravitino superWIMP scenario differs markedly from other gravitino dark matter scenarios. In previous frameworks (68; 76; 63; 65; 62; 34; 35; 60; 33; 64; 14), gravitinos were expected to be produced either thermally, with  $\Omega_{\tilde{G}} \sim 0.1$  obtained by requiring  $m_{\tilde{G}} \sim \text{keV}$ , or through reheating, with  $\Omega_{\tilde{G}} \sim 0.1$  obtained by tuning the reheat temperature to  $T_{\text{RH}} \sim 10^{10}$  GeV. In the superWIMP scenario, the desired amount of dark matter is obtained without relying on the introduction of new, fine-tuned energy scales.

Other examples of superWIMPs include Kaluza-Klein gravitons in scenarios with universal extra dimensions (44; 45; 43), axinos (70; 22; 21) and quintessinos (12; 13) in supersymmetric theories, and many other scenarios in which a metastable particle decays to the true dark matter particle through highly suppressed interactions, with lifetimes ranging from fractions of a second to beyond the age of the Universe.

### 10.2.2 Astrophysical Signals

Because superWIMPs are very weakly interacting, they are impossible to detect in conventional direct and indirect dark matter search experiments. At the same time, the extraordinarily weak couplings of superWIMPs imply that the decays of WIMPs to superWIMPs may be very late and have an observable impact on, for example, Big Bang nucleosynthesis (BBN), the Planckian spectrum of the cosmic microwave background (CMB), small scale structure, the diffuse photon flux, and cosmic ray experiments.

In the prototypical case of a slepton decaying to a gravitino superWIMP, the decay width is

$$\Gamma(\tilde{l} \rightarrow l\tilde{G}) = \frac{1}{48\pi M_*^2} \frac{m_{\tilde{l}}^5}{m_{\tilde{G}}^2} \left[ 1 - \frac{m_{\tilde{G}}^2}{m_{\tilde{l}}^2} \right]^4, \quad (10.4)$$

assuming the lepton mass is negligible. This decay width depends on only the slepton mass, the gravitino mass, and the Planck mass. For  $m_{\tilde{G}}/m_{\tilde{l}} \approx 1$ , the slepton decay lifetime is

$$\tau(\tilde{l} \rightarrow l\tilde{G}) \simeq 3.6 \times 10^8 \text{ s} \left[ \frac{100 \text{ GeV}}{m_{\tilde{l}} - m_{\tilde{G}}} \right]^4 \left[ \frac{m_{\tilde{G}}}{\text{TeV}} \right]. \quad (10.5)$$

This expression is valid only when the gravitino and slepton are nearly degenerate, but usefully illustrates that decay lifetimes of the order of days or months are perfectly natural. Similar expressions hold for the decay of a neutralino NLSP to a gravitino.

#### 10.2.2.1 BBN and CMB

Signals in BBN and the CMB are determined primarily by the WIMP lifetime and the energy released in visible decay products when the WIMP decays. This energy release destroys and creates light elements, distorting the predictions of standard BBN. In addition, the injection of electromagnetic energy may also distort the frequency dependence of the CMB away from its ideal black body spectrum. For the decay times of interest with redshifts  $z \sim 10^5$  to  $10^7$ , the resulting photons interact efficiently through  $\gamma e^- \rightarrow \gamma e^-$  and  $eX \rightarrow eX\gamma$ , where  $X$  is an ion, but photon number is conserved, since double Compton scattering  $\gamma e^- \rightarrow \gamma\gamma e^-$  is inefficient. The spectrum therefore relaxes to statistical but not thermodynamic equilibrium, resulting in a Bose-Einstein distribution function

$$f_\gamma(E) = \frac{1}{e^{E/(kT)+\mu} - 1}, \quad (10.6)$$

with chemical potential  $\mu \neq 0$ .

The energy release is conveniently expressed in terms of

$$\xi_{\text{EM}} \equiv \epsilon_{\text{EM}} B_{\text{EM}} Y_{\text{NLSP}} \quad (10.7)$$

for electromagnetic energy, with a similar expression for hadronic energy. Here  $\epsilon_{\text{EM}}$  is the initial EM energy released in NLSP decay, and  $B_{\text{EM}}$  is the branching fraction of NLSP decay into EM components.  $Y_{\text{NLSP}} \equiv n_{\text{NLSP}}/n_\gamma$  is the NLSP number density just before NLSP decay, normalized to the

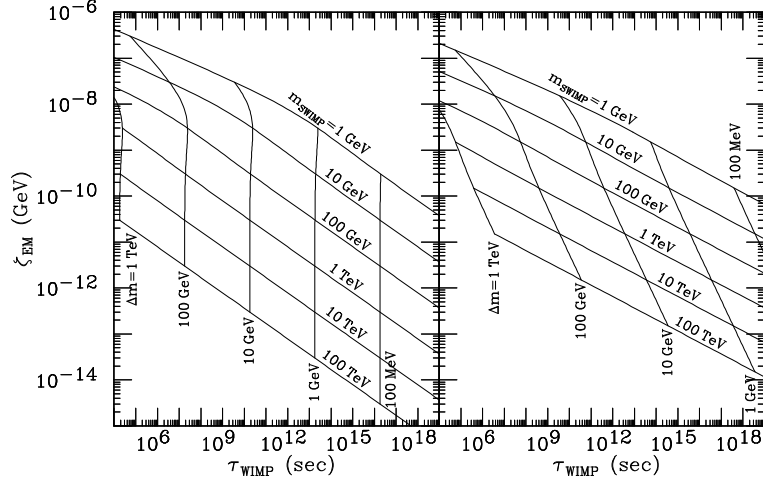


Fig. 10.2. Predicted values of WIMP lifetime  $\tau$  and electromagnetic energy release  $\zeta_{\text{EM}} \equiv \varepsilon_{\text{EM}} Y_{\text{WIMP}}$  in the  $\tilde{B}$  (left) and  $\tilde{\tau}$  (right) NLSP scenarios for  $m_{\text{SWIMP}} = 1 \text{ GeV}, 10 \text{ GeV}, \dots, 100 \text{ TeV}$  (top to bottom) and  $\Delta m \equiv m_{\text{WIMP}} - m_{\text{SWIMP}} = 1 \text{ TeV}, 100 \text{ GeV}, \dots, 100 \text{ MeV}$  (left to right). For the  $\tilde{\tau}$  NLSP scenario, we assume  $\varepsilon_{\text{EM}} = \frac{1}{2} E_{\tilde{\tau}}$ . From Ref. (45).

background photon number density  $n_{\gamma} = 2\zeta(3)T^3/\pi^2$ . It can be expressed in terms of the superWIMP abundance:

$$Y_{\text{NLSP}} \simeq 3.0 \times 10^{-12} \left[ \frac{\text{TeV}}{m_{\tilde{G}}} \right] \left[ \frac{\Omega_{\tilde{G}}}{0.23} \right]. \quad (10.8)$$

Once an NLSP candidate is specified, and assuming superWIMPs make up all of the dark matter, with  $\Omega_{\tilde{G}} = \Omega_{\text{DM}} = 0.23$ , both the lifetime and energy release are determined by only two parameters:  $m_{\tilde{G}}$  and  $m_{\text{NLSP}}$ . The results for slepton and neutralino NLSPs are given in Fig. 10.2.

In Fig. 10.3, these predictions are compared with BBN and CMB constraints. The shaded regions are excluded by an analysis of BBN constraints on EM energy release (24). This analysis has been strengthened by including hadronic constraints and updated and refined in many ways in recent years, as described in Chapter 28. Although the excluded region has shifted around, the basic features remain: some of the gravitino superWIMP parameter space is excluded, and some remains. In addition, late decays to superWIMPs may in fact improve the current disagreement of standard BBN predictions with the observed  ${}^7\text{Li}$  and  ${}^6\text{Li}$  abundances (23; 9).

Figure 10.3 also includes contours of the chemical potential  $\mu$ , as determined by updating the analysis of Ref. (58). The current bound is

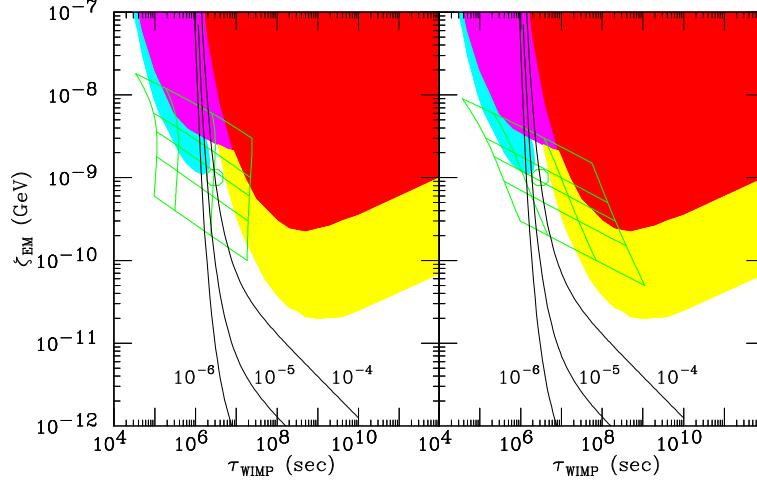


Fig. 10.3. The grid gives predicted values of WIMP lifetime  $\tau$  and electromagnetic energy release  $\zeta_{\text{EM}} \equiv \varepsilon_{\text{EM}} Y_{\text{WIMP}}$  in the  $\tilde{B}$  (left) and  $\tilde{\tau}$  (right) WIMP scenarios for  $m_{\text{SWIMP}} = 100$  GeV, 300 GeV, 500 GeV, 1 TeV, and 3 TeV (top to bottom) and  $\Delta m \equiv m_{\text{WIMP}} - m_{\text{SWIMP}} = 600$  GeV, 400 GeV, 200 GeV, and 100 GeV (left to right). For the  $\tilde{\tau}$  WIMP scenario, we assume  $\varepsilon_{\text{EM}} = \frac{1}{2} E_{\tau}$ . The shaded regions are excluded in one analysis of BBN constraints (24); the circle gives a region in which  ${}^7\text{Li}$  is reduced to observed levels. The contours are for  $\mu$ , which parameterizes the distortion of the CMB from a Planckian spectrum. From Ref. (45).

$\mu < 9 \times 10^{-5}$  (52; 32). Although there are at present no indications of deviations from black body, current limits are already sensitive to the superWIMP scenario, and future improvements will further probe superWIMP parameter space.

#### 10.2.2.2 Small Scale Structure

In contrast to WIMPs, superWIMPs are produced with large velocities at late times. This has two effects. First, the velocity dispersion reduces the phase space density, smoothing out cusps in DM halos. Second, such particles damp the linear power spectrum, reducing power on small scales (19; 61; 15).

Depending on the particular decay time and decay kinematics, superWIMPs may be cold or warm. As seen in Fig. 10.4, superWIMPs may suppress small scale structure as effectively as a 1 keV sterile neutrino. Some superWIMP scenarios may therefore be differentiated from standard cold DM scenarios by studies of halo profiles, and may even be favored by indications that cold DM predicts halos that are too cuspy, as discussed in Chapter 3.

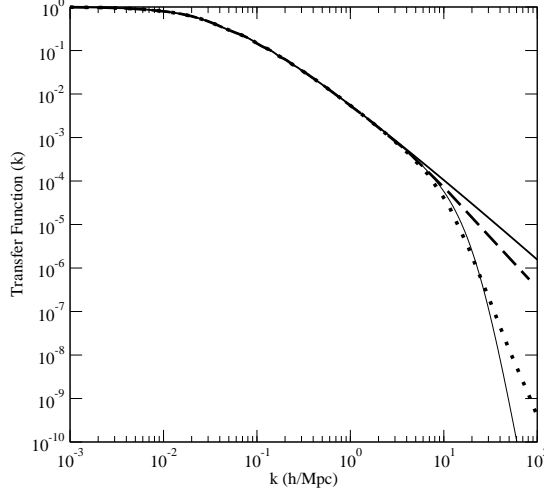


Fig. 10.4. The power spectrum for scenarios in which dark matter is completely composed of WIMPs (solid), half WIMPs and half superWIMPs (dashed), and completely composed of superWIMPs (dotted). For comparison, the this solid curve is the transfer function for a 1 keV warm DM model. From Ref. (61).

### 10.2.3 Astroparticle and Collider Signals

The possibility of long-lived charged particles in superWIMP scenarios also has many implications for astroparticle and particle physics experiments.

#### 10.2.3.1 Cosmic Rays

In superWIMP (and other similar) scenarios, long-lived charged particles may be produced by cosmic rays, resulting in exotic signals in cosmic ray and cosmic neutrino experiments (3; 13; 4; 1; 7; 5; 18). As an example, ultra-high energy neutrinos may produce events with two long-lived sleptons through  $\nu q \rightarrow \tilde{l} \tilde{q}'$  followed by the decay  $\tilde{q}' \rightarrow \tilde{l}$ . The sleptons are metastable and propagate to neutrino telescopes (59), where they have a typical transverse separation of hundreds of meters. They may therefore be detected above background as events with two upward-going, extremely high energy charged tracks in experiments such as IceCube.

#### 10.2.3.2 Colliders

As evident in Eq. (10.5), in supersymmetric superWIMP scenarios, the NLSP decays to the gravitino with lifetimes that may be of the order of

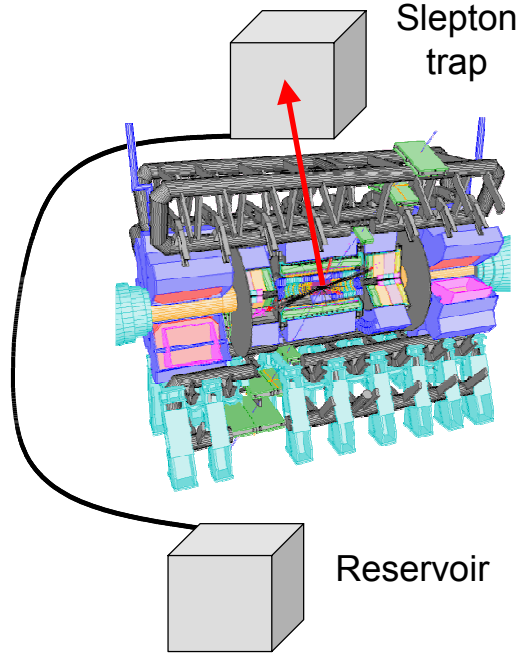


Fig. 10.5. Configuration for slepton trapping in gravitino superWIMP scenarios. From Ref. (47).

seconds to months. Such particles are effectively stable in collider experiments, and this scenario therefore implies that each supersymmetric event will be characterized not by missing energy, but by two charged, heavy metastable particles. This is a spectacular signal that will be cannot escape notice at the LHC (31; 53; 67; 42; 50). In addition, given the possibility of long lifetimes, it suggests that decays to gravitinos may be observed by capturing slepton NLSPs and detecting their decays.

The sleptons may be captured in water tanks placed outside collider detectors (47), in the detectors themselves (55), or by mining LHC cavern walls for sleptons (25). In the first case, shown in Fig. 10.5, the water tanks may be drained periodically to underground reservoirs where slepton decays may be observed in quiet environments. As many as  $10^4$  sleptons per year may be stopped in 1 meter thick water tanks, opening up the possibility of a precise measurement of slepton lifetime and the first study of a gravitational process at high energy colliders, along with many other implications (46).



### 10.3 WIMPlless Dark Matter

#### 10.3.1 Candidates and Relic Densities

Under general conditions, the thermal relic density of a particle  $X$  is (77; 20; 74; 73)

$$\Omega_X \propto \frac{1}{\langle \sigma v \rangle} \sim \frac{m_X^2}{g_X^4}, \quad (10.9)$$

where  $\langle \sigma v \rangle$  is its thermally-averaged annihilation cross section, and  $m_X$  and  $g_X$  are the characteristic mass scale and coupling entering this cross section. The last step follows from dimensional analysis. The WIMP miracle is the statement that, for  $m_X \sim m_{\text{weak}} \sim 100 \text{ GeV} - 1 \text{ TeV}$  and  $g_X \sim g_{\text{weak}} \simeq 0.65$ ,  $\Omega_X$  is roughly  $\Omega_{\text{DM}} \approx 0.23$ .

Equation (10.9) makes clear, however, that the thermal relic density fixes only one combination of the dark matter's mass and coupling, and other combinations of  $(m_X, g_X)$  can also give the correct  $\Omega_X$ . WIMPlless models (39) are those in which the correct thermal relic density is achieved with parameters  $(m_X, g_X) \neq (m_{\text{weak}}, g_{\text{weak}})$ .

Because WIMPlless dark matter does not have weak interactions, and existing constraints effectively exclude electromagnetic and strong interactions, WIMPlless dark matter is necessarily hidden dark matter, that is, dark matter that has no standard model gauge interactions. Hidden sectors have a long history, and hidden sector dark matter has been discussed for decades, beginning with work on mirror matter and related ideas. For a general discussion and references, see Chapter 9. Here we note only that, counter to conventional wisdom, existing constraints place only weak bounds on hidden sectors. For example, light degrees of freedom change the expansion rate of the Universe and thereby impact BBN. The constraint from BBN is highly sensitive to the temperature of the hidden sector, however. Current bounds from BBN on the number of light and heavy degrees of freedom are given in Fig. 10.6. For hidden sector temperatures within a factor of 2 of the observable sector, hundreds of degrees of freedom, equivalent to several copies of the standard model or the minimal supersymmetric standard model (MSSM), may be accommodated.

Of course, WIMPlless dark matter requires hidden sectors with additional structure to guarantee that the hidden sector's dark matter has the desired thermal relic density. Remarkably, this structure may be found in well-motivated models that have been explored previously for many other reasons (39). As an example, consider supersymmetric models with gauge-mediated supersymmetry breaking (GMSB) (28; 27; 66; 6; 30; 29). These models necessarily have several sectors, as shown in Fig. 10.7. The supersymmetry-

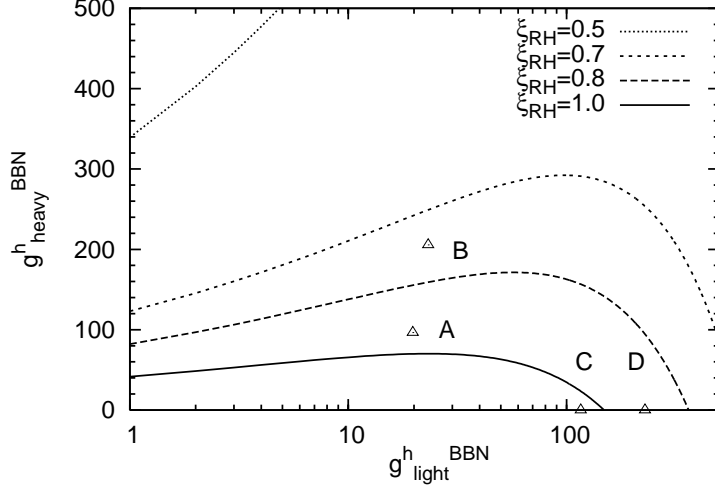


Fig. 10.6. Bounds from BBN in the  $(g_{\text{light}}^{h \text{ BBN}}, g_{\text{heavy}}^{h \text{ BBN}})$  plane, where  $g_{\text{light}}^{h \text{ BBN}}$  and  $g_{\text{heavy}}^{h \text{ BBN}}$  are the hidden degrees of freedom with masses  $m < T_{\text{BBN}}^h$  and  $T_{\text{BBN}}^h < m < T_{\text{RH}}^h$ , respectively, for hidden to observable sector reheat temperature ratios  $T_{\text{RH}}^h/T_{\text{RH}} = 0.5, 0.7, 0.8, 1.0$  (from top to bottom). The regions above the contours are excluded. The values of  $(g_{\text{light}}^{h \text{ BBN}}, g_{\text{heavy}}^{h \text{ BBN}})$  are marked for four example hidden sectors: (A) 1-generation and (B) 3-generation flavor-free versions of the MSSM with  $T_{\text{BBN}}^h < m_X < T_{\text{RH}}^h$ , and (C) 1-generation and (D) 3-generation flavor-free versions of the MSSM with  $m_X < T_{\text{BBN}}^h/2$ . From Ref. (51).

breaking sector includes the fields that break supersymmetry dynamically and mediate this breaking to other sectors through gauge interactions. The MSSM sector includes the fields of the minimal supersymmetric standard model. In addition, supersymmetry breaking may also be mediated to one or more hidden sectors. The hidden sectors are not strictly necessary, but given the discussion above, there is no reason to prevent them, and hidden sectors are ubiquitous in such models originating in string theory.

As is well-known, GMSB models generate superpartner masses proportional to gauge couplings squared. Slightly more precisely, the MSSM superpartner masses are

$$m \sim \frac{g^2}{16\pi^2} \frac{F}{M}, \quad (10.10)$$

where  $g$  is the largest relevant standard model gauge coupling, and  $F$  and  $M$  are the vacuum expectation values of the supersymmetry-breaking sector's chiral field  $S$ , with  $\langle S \rangle = M + \theta^2 F$ . With analogous couplings of the hidden sector fields to hidden messengers, the hidden sector superpartner masses

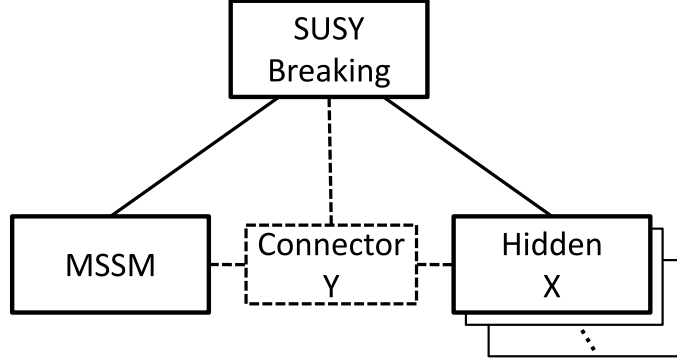


Fig. 10.7. Sectors of supersymmetric models. Supersymmetry breaking is mediated by gauge interactions to the MSSM and the hidden sector, which contains the dark matter particle  $X$ . An optional connector sector contains fields  $Y$ , charged under both MSSM and hidden sector gauge groups, which induce signals in direct and indirect searches and at colliders. There may also be other hidden sectors, leading to multi-component dark matter. From Ref. (39).

are

$$m_X \sim \frac{g_X^2}{16\pi^2} \frac{F}{M}, \quad (10.11)$$

where  $g_X$  is the relevant hidden sector gauge coupling. As a result,

$$\frac{m_X}{g_X^2} \sim \frac{m}{g^2} \sim \frac{F}{16\pi^2 M}; \quad (10.12)$$

that is,  $m_X/g_X^2$  is determined solely by the supersymmetry-breaking sector. As this is exactly the combination of parameters that determines the thermal relic density of Eq. (10.9), the hidden sector automatically includes a dark matter candidate that has the desired thermal relic density, irrespective of its mass.

The freeze out of hidden sector dark matter in such GMSB models has been studied numerically. As an example, in Ref. (51) the hidden sector was assumed to be a copy of the MSSM, but with a free superpartner mass scale  $m_X$  and all Yukawa couplings  $\sim \mathcal{O}(1)$ , so that the only light hidden sector particles are the hidden gluon, photon, and neutrinos. The results are given in Fig. 10.8. The criterion that the standard model weak scale be between 100 GeV and 1 TeV requires values of  $(m_X, g_X)$  within the band. The solid curves, where the thermal relic density of hidden dark matter is consistent with dark matter, are seen to lie within this band, confirming the scaling arguments and rough estimates described above.

In summary, well-known frameworks for hidden sectors include models

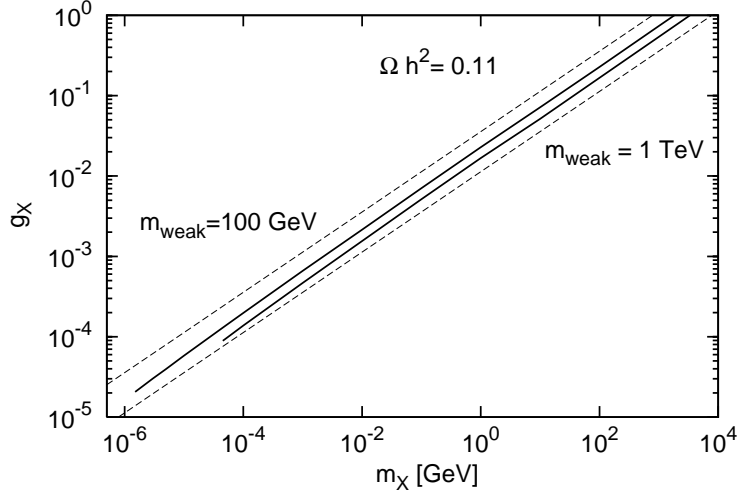


Fig. 10.8. Contours of  $\Omega_X h^2 = 0.11$  in the  $(m_X, g_X)$  plane for hidden to observable reheat temperature ratios  $T_{\text{RH}}^h/T_{\text{RH}} = 0.8$  (upper solid) and  $0.3$  (lower solid), where the hidden sector is a 1-generation flavor-free version of the MSSM. Also plotted are lines of  $m_{\text{weak}} \equiv (m_X/g_X^2)g'^2 = 100$  GeV (upper dashed) and  $1$  TeV (lower dashed). From Ref. (51).

in which the hidden sector contains a particle whose thermal relic density is automatically in the desired range to be dark matter, even when the particle's mass is not at the weak scale. This property relies on the relation  $m_X \propto g_X^2$ , which is common to other frameworks for new physics that avoid flavor-changing problems, such as anomaly-mediated supersymmetry breaking. The “coincidence” required for WIMPless dark matter may also be found in other settings; see, for example, Ref. (57).

### 10.3.2 Direct and Indirect Detection Signals

The decoupling of the WIMP miracle from WIMPs has many possible implications and observable consequences. In the case that the dark matter is truly hidden, it implies that there are no prospects for direct or indirect detection. Signals must be found in astrophysical observations, as in the case of superWIMPs. Alternatively, there may be connector sectors containing particles that mediate interactions between the standard model and the hidden sector through non-gauge (Yukawa) interactions (see Fig. 10.7). Such connectors may generate many signals with energies and rates typically unavailable to WIMPs.

As an example, first consider direct detection. The DAMA signal, inter-

puted as spin-independent, elastic scattering, has conventionally favored a region in the mass-cross section plane with  $(m_X, \sigma_{\text{SI}}) \sim (20\text{--}200 \text{ GeV}, 10^{-5} \text{ pb})$  (10). This is now excluded, most stringently by XENON10 (8) and CDMS (Ge) (2), which require  $\sigma_{\text{SI}} < 10^{-7} \text{ pb}$  throughout this range of  $m_X$ . Gondolo and Gelmini have noted, however, that an alternative region with  $(m_X, \sigma_{\text{SI}}) \sim (1\text{--}10 \text{ GeV}, 10^{-3} \text{ pb})$  may explain the DAMA results without violating other known bounds (54). DAMA's relative sensitivity to this region follows from its low energy threshold and the lightness of Na nuclei. This region may be extended to lower masses and cross sections by the effects of channeling (11; 69; 16; 72; 38) and may also be broadened by dark matter streams in the solar neighborhood (54).

The acceptable DAMA-favored region with  $m_X \sim 5 \text{ GeV}$  has masses that are low for WIMPs, given that their masses are expected to be around  $m_{\text{weak}} \sim 100 \text{ GeV} - 1 \text{ TeV}$ . However, in WIMPless models, where the thermal relic density is achieved for a variety of dark matter masses, such masses are perfectly natural. A WIMPless particle  $X$  may couple to the standard model through Yukawa interactions

$$\mathcal{L} = \lambda_f X \bar{Y}_L f_L + \lambda_f X \bar{Y}_R f_R, \quad (10.13)$$

where  $Y$  is a vector-like connector fermion, and  $f$  is a standard model fermion. Taking  $f$  to be the  $b$  quark, and the  $Y$  mass to be 400 GeV, consistent with current bounds, these couplings generate spin-independent scattering cross sections given in Fig. 10.9. We see that WIMPless dark matter may explain the DAMA results without difficulty.

WIMPless dark matter also provides new target signals for indirect detection. For WIMPs, annihilation cross sections determine both the thermal relic density and indirect detection signals. The thermal relic density therefore constrains the rates of indirect detection signals. In the WIMPless case, however, this connection is weakened, since the thermal relic density is governed by hidden sector annihilation and gauge interactions, while the indirect detection signals are governed by the interactions of Eq. (10.13).

This provides a wealth of new opportunities for indirect detection. As an example, WIMPless dark matter may be detected through its annihilation to neutrinos in the Sun by experiments such as Super-Kamiokande. Although such rates depend on the competing cross sections for capture and annihilation, the Sun has almost certainly reached its equilibrium state, and the annihilation rate is determined by the scattering cross section (26). The prospects for Super-Kamiokande may therefore be compared to direct detection rates (26; 56; 40). The results are given in Fig. 10.9. In the

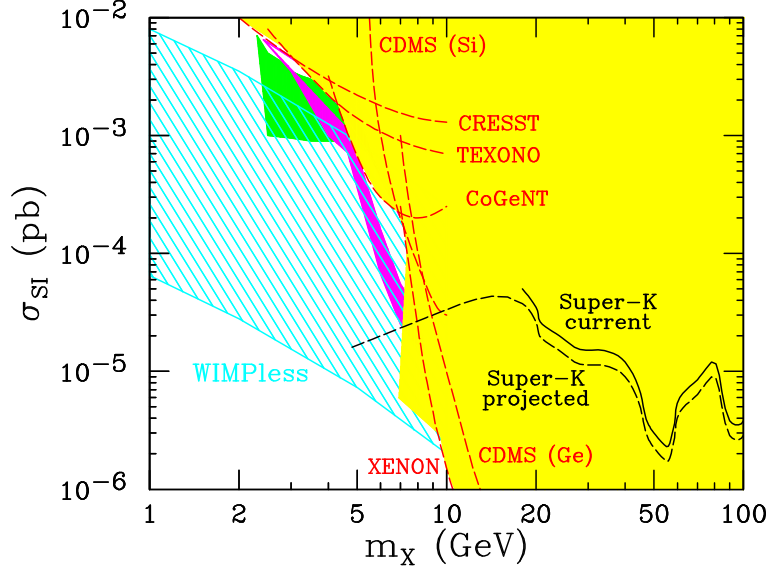


Fig. 10.9. Direct detection cross sections for spin-independent  $X$ -nucleon scattering as a function of dark matter mass  $m_X$ . The magenta shaded region is DAMA-favored given channeling and no streams (69), and the medium green shaded region is DAMA-favored at  $3\sigma$  given streams and no channeling (54). The light yellow shaded region is excluded by the direct detection experiments indicated. The blue cross-hatched region is the parameter space of WIMPless models with connector mass  $m_Y = 400$  GeV and  $0.3 < \lambda_b < 1.0$ . The black solid line is the published Super-K exclusion limit (26), and the black dashed line is a projection of future Super-K sensitivity. From Ref. (40).

near future, Super-Kamiokande may be able to probe the low mass regions corresponding to the DAMA signal.

WIMPless dark matter also provides additional targets for indirect detection experiments looking for photons, positrons, and other annihilation products. The connectors may also play an interesting role in collider experiments. Further details may be found in Refs. (41; 56; 40).

## Bibliography

- [1] Markus Ahlers, Joern Kersten, and Andreas Ringwald. Long-lived staus at neutrino telescopes. *JCAP*, 0607:005, 2006, hep-ph/0604188.
- [2] Z. Ahmed et al. A Search for WIMPs with the First Five-Tower Data from CDMS. 2008, arXiv:0802.3530 [astro-ph].
- [3] Ivone Albuquerque, Gustavo Burdman, and Z. Chacko. Neutrino telescopes as a direct probe of supersymmetry breaking. *Phys. Rev. Lett.*, 92:221802, 2004, hep-ph/0312197.
- [4] Ivone F. M. Albuquerque, Gustavo Burdman, and Z. Chacko. Direct Detection of Supersymmetric Particles in Neutrino Telescopes. *Phys. Rev.*, D75:035006, 2007, hep-ph/0605120.
- [5] Ivone F. M. Albuquerque, Gustavo Burdman, Christopher A. Krenke, and Baran Nosratpour. Direct Detection of Kaluza-Klein Particles in Neutrino Telescopes. *Phys. Rev.*, D78:015010, 2008, arXiv:0803.3479 [hep-ph].
- [6] Luis Alvarez-Gaume, Mark Claudson, and Mark B. Wise. Low-Energy Supersymmetry. *Nucl. Phys.*, B207:96, 1982.
- [7] Shin’ichiro Ando, John F. Beacom, Stefano Profumo, and David Rainwater. Probing new physics with long-lived charged particles produced by atmospheric and astrophysical neutrinos. *JCAP*, 0804:029, 2008, arXiv:0711.2908 [hep-ph].
- [8] J. Angle et al. First Results from the XENON10 Dark Matter Experiment at the Gran Sasso National Laboratory. *Phys. Rev. Lett.*, 100:021303, 2008, arXiv:0706.0039 [astro-ph].
- [9] Sean Bailly, Karsten Jedamzik, and Gilbert Moulhaka. Gravitino Dark Matter and the Cosmic Lithium Abundances. 2008, arXiv:0812.0788 [hep-ph].
- [10] P. Belli et al. Extending the DAMA annual-modulation region by

- inclusion of the uncertainties in astrophysical velocities. *Phys. Rev.*, D61:023512, 2000, hep-ph/9903501.
- [11] R. Bernabei et al. Possible implications of the channeling effect in NaI(Tl) crystals. *Eur. Phys. J.*, C53:205–213, 2008, arXiv:0710.0288 [astro-ph].
  - [12] Xiao-Jun Bi, Ming-zhe Li, and Xin-min Zhang. Quintessino as dark matter. *Phys. Rev.*, D69:123521, 2004, hep-ph/0308218.
  - [13] Xiao-Jun Bi, Jian-Xiong Wang, Chao Zhang, and Xin-min Zhang. Phenomenology of quintessino dark matter. *Phys. Rev.*, D70:123512, 2004, hep-ph/0404263.
  - [14] M. Bolz, A. Brandenburg, and W. Buchmuller. Thermal Production of Gravitinos. *Nucl. Phys.*, B606:518–544, 2001, hep-ph/0012052.
  - [15] Francesca Borzumati, Torsten Bringmann, and Piero Ullio. Dark matter from late decays and the small-scale structure problems. *Phys. Rev.*, D77:063514, 2008, hep-ph/0701007.
  - [16] A. Bottino, F. Donato, N. Fornengo, and S. Scopel. Interpreting the recent results on direct search for dark matter particles in terms of relic neutralino. *Phys. Rev.*, D78:083520, 2008, arXiv:0806.4099 [hep-ph].
  - [17] Wilfried Buchmuller, Koichi Hamaguchi, Michael Ratz, and Tsutomu Yanagida. Supergravity at colliders. *Phys. Lett.*, B588:90–98, 2004, hep-ph/0402179.
  - [18] B. Canadas, D. G. Cerdeno, C. Munoz, and S. Panda. Stau detection at neutrino telescopes in scenarios with supersymmetric dark matter. 2008, arXiv:0812.1067 [hep-ph].
  - [19] Jose A. R. Cembranos, Jonathan L. Feng, Arvind Rajaraman, and Fumihiro Takayama. SuperWIMP solutions to small scale structure problems. *Phys. Rev. Lett.*, 95:181301, 2005, hep-ph/0507150.
  - [20] Hong-Yee Chiu. Symmetry between particle and anti-particle populations in the universe. *Phys. Rev. Lett.*, 17:712, 1966.
  - [21] Laura Covi, Hang-Bae Kim, Jihn E. Kim, and Leszek Roszkowski. Axinos as dark matter. *JHEP*, 05:033, 2001, hep-ph/0101009.
  - [22] Laura Covi, Jihn E. Kim, and Leszek Roszkowski. Axinos as cold dark matter. *Phys. Rev. Lett.*, 82:4180–4183, 1999, hep-ph/9905212.
  - [23] Daniel Cumberbatch et al. Solving the cosmic lithium problems with primordial late- decaying particles. *Phys. Rev.*, D76:123005, 2007, arXiv:0708.0095 [astro-ph].
  - [24] Richard H. Cyburt, John R. Ellis, Brian D. Fields, and Keith A. Olive. Updated nucleosynthesis constraints on unstable relic particles. *Phys. Rev.*, D67:103521, 2003, astro-ph/0211258.



- [25] A. De Roeck et al. Supersymmetric benchmarks with non-universal scalar masses or gravitino dark matter. *Eur. Phys. J.*, C49:1041–1066, 2007, hep-ph/0508198.
- [26] S. Desai et al. Search for dark matter WIMPs using upward through-going muons in Super-Kamiokande. *Phys. Rev.*, D70:083523, 2004, hep-ex/0404025.
- [27] Savas Dimopoulos and Stuart Raby. Supercolor. *Nucl. Phys.*, B192:353, 1981.
- [28] Michael Dine, Willy Fischler, and Mark Srednicki. Supersymmetric Technicolor. *Nucl. Phys.*, B189:575–593, 1981.
- [29] Michael Dine, Ann E. Nelson, Yosef Nir, and Yuri Shirman. New tools for low-energy dynamical supersymmetry breaking. *Phys. Rev.*, D53:2658–2669, 1996, hep-ph/9507378.
- [30] Michael Dine, Ann E. Nelson, and Yuri Shirman. Low-energy dynamical supersymmetry breaking simplified. *Phys. Rev.*, D51:1362–1370, 1995, hep-ph/9408384.
- [31] Manuel Drees and X. Tata. Signals for heavy exotics at hadron colliders and supercolliders. *Phys. Lett.*, B252:695–702, 1990.
- [32] S. Eidelman et al. Review of particle physics. *Phys. Lett.*, B592:1, 2004.
- [33] John R. Ellis, G. B. Gelmini, Jorge L. Lopez, Dimitri V. Nanopoulos, and Subir Sarkar. Astrophysical constraints on massive unstable neutral relic particles. *Nucl. Phys.*, B373:399–437, 1992.
- [34] John R. Ellis, Jihn E. Kim, and Dimitri V. Nanopoulos. Cosmological Gravitino Regeneration and Decay. *Phys. Lett.*, B145:181, 1984.
- [35] John R. Ellis, Dimitri V. Nanopoulos, and Subir Sarkar. The Cosmology of Decaying Gravitinos. *Nucl. Phys.*, B259:175, 1985.
- [36] John R. Ellis, Keith A. Olive, Yudi Santoso, and Vassilis C. Spanos. Gravitino dark matter in the CMSSM. *Phys. Lett.*, B588:7–16, 2004, hep-ph/0312262.
- [37] John R. Ellis, Keith A. Olive, Yudi Santoso, and Vassilis C. Spanos. Prospects for sparticle discovery in variants of the MSSM. *Phys. Lett.*, B603:51, 2004, hep-ph/0408118.
- [38] Malcolm Fairbairn and Thomas Schwetz. Spin-independent elastic WIMP scattering and the DAMA annual modulation signal. 2008, arXiv:0808.0704 [hep-ph].
- [39] Jonathan L. Feng and Jason Kumar. The WIMPless Miracle: Dark-Matter Particles without Weak- Scale Masses or Weak Interactions. *Phys. Rev. Lett.*, 101:231301, 2008, arXiv:0803.4196 [hep-ph].
- [40] Jonathan L. Feng, Jason Kumar, John Learned, and Louis E. Strigari.

- Testing the Dark Matter Interpretation of the DAMA/LIBRA Result with Super-Kamiokande. 2008, arXiv:0808.4151 [hep-ph].
- [41] Jonathan L. Feng, Jason Kumar, and Louis E. Strigari. Explaining the DAMA Signal with WIMPless Dark Matter. *Phys. Lett.*, B670:37–40, 2008, arXiv:0806.3746 [hep-ph].
  - [42] Jonathan L. Feng and Takeo Moroi. Tevatron signatures of long-lived charged sleptons in gauge-mediated supersymmetry breaking models. *Phys. Rev.*, D58:035001, 1998, hep-ph/9712499.
  - [43] Jonathan L. Feng, Arvind Rajaraman, and Fumihiro Takayama. Graviton cosmology in universal extra dimensions. *Phys. Rev.*, D68:085018, 2003, hep-ph/0307375.
  - [44] Jonathan L. Feng, Arvind Rajaraman, and Fumihiro Takayama. Superweakly-interacting massive particles. *Phys. Rev. Lett.*, 91:011302, 2003, hep-ph/0302215.
  - [45] Jonathan L. Feng, Arvind Rajaraman, and Fumihiro Takayama. SuperWIMP Dark Matter Signals from the Early Universe. *Phys. Rev.*, D68:063504, 2003, hep-ph/0306024.
  - [46] Jonathan L. Feng, Arvind Rajaraman, and Fumihiro Takayama. Probing gravitational interactions of elementary particles. *Int. J. Mod. Phys.*, D13:2355–2359, 2004, hep-th/0405248.
  - [47] Jonathan L. Feng and Bryan T. Smith. Slepton trapping at the Large Hadron and International Linear Colliders. *Phys. Rev.*, D71:015004, 2005, hep-ph/0409278.
  - [48] Jonathan L. Feng, Shu-fang Su, and Fumihiro Takayama. SuperWIMP gravitino dark matter from slepton and sneutrino decays. *Phys. Rev.*, D70:063514, 2004, hep-ph/0404198.
  - [49] Jonathan L. Feng, Shufang Su, and Fumihiro Takayama. Supergravity with a gravitino LSP. *Phys. Rev.*, D70:075019, 2004, hep-ph/0404231.
  - [50] Jonathan L. Feng, Shufang Su, and Fumihiro Takayama. Lower limit on dark matter production at the Large Hadron Collider. *Phys. Rev. Lett.*, 96:151802, 2006, hep-ph/0503117.
  - [51] Jonathan L. Feng, Huitzu Tu, and Hai-Bo Yu. Thermal Relics in Hidden Sectors. *JCAP*, 0810:043, 2008, arXiv:0808.2318 [hep-ph].
  - [52] D. J. Fixsen et al. The Cosmic Microwave Background Spectrum from the Full COBE/FIRAS Data Set. *Astrophys. J.*, 473:576, 1996, astro-ph/9605054.
  - [53] J. L. Goity, W. J. Kossler, and Marc Sher. Production, collection and utilization of very longlived heavy charged leptons. *Phys. Rev.*, D48:5437–5439, 1993, hep-ph/9305244.

- [54] Paolo Gondolo and Graciela Gelmini. Compatibility of DAMA dark matter detection with other searches. *Phys. Rev.*, D71:123520, 2005, hep-ph/0504010.
- [55] Koichi Hamaguchi, Yoshitaka Kuno, Tsuyoshi Nakaya, and Mihoko M. Nojiri. A study of late decaying charged particles at future colliders. *Phys. Rev.*, D70:115007, 2004, hep-ph/0409248.
- [56] Dan Hooper, Frank Petriello, Kathryn M. Zurek, and Marc Kamionkowski. The New DAMA Dark-Matter Window and Energetic-Neutrino Searches. 2008, arXiv:0808.2464 [hep-ph].
- [57] Dan Hooper and Kathryn M. Zurek. Natural supersymmetric model with MeV dark matter. *Phys. Rev.*, D77:087302, 2008, arXiv:0801.3686 [hep-ph].
- [58] W. Hu and J. Silk. Thermalization constraints and spectral distortions for massive unstable relic particles. *Phys. Rev. Lett.*, 70:2661–2664, 1993.
- [59] Yiwen Huang, Mary Hall Reno, Ina Sarcevic, and Jessica Uscinski. Weak interactions of supersymmetric staus at high energies. *Phys. Rev.*, D74:115009, 2006, hep-ph/0607216.
- [60] R. Juszkiewicz, J. Silk, and A. Stebbins. Constraints on Cosmologically Regenerated Gravitinos. *Phys. Lett.*, B158:463–467, 1985.
- [61] Manoj Kaplinghat. Dark matter from early decays. *Phys. Rev.*, D72:063510, 2005, astro-ph/0507300.
- [62] M. Yu. Khlopov and Andrei D. Linde. Is It Easy to Save the Gravitino? *Phys. Lett.*, B138:265–268, 1984.
- [63] Lawrence M. Krauss. New Constraints on Ino Masses from Cosmology. 1. Supersymmetric Inos. *Nucl. Phys.*, B227:556, 1983.
- [64] T. Moroi, H. Murayama, and Masahiro Yamaguchi. Cosmological constraints on the light stable gravitino. *Phys. Lett.*, B303:289–294, 1993.
- [65] Dimitri V. Nanopoulos, Keith A. Olive, and M. Srednicki. After Primordial Inflation. *Phys. Lett.*, B127:30, 1983.
- [66] Chiara R. Nappi and Burt A. Ovrut. Supersymmetric Extension of the  $SU(3) \times SU(2) \times U(1)$  Model. *Phys. Lett.*, B113:175, 1982.
- [67] Aleandro Nisati, Silvano Petrarca, and Giorgio Salvini. On the possible detection of massive stable exotic particles at the LHC. *Mod. Phys. Lett.*, A12:2213–2222, 1997, hep-ph/9707376.
- [68] Heinz Pagels and Joel R. Primack. Supersymmetry, Cosmology and New TeV Physics. *Phys. Rev. Lett.*, 48:223, 1982.
- [69] Frank Petriello and Kathryn M. Zurek. DAMA and WIMP dark matter. *JHEP*, 09:047, 2008, arXiv:0806.3989 [hep-ph].

- [70] Krishna Rajagopal, Michael S. Turner, and Frank Wilczek. Cosmological implications of axinos. *Nucl. Phys.*, B358:447–470, 1991.
- [71] Leszek Roszkowski, Roberto Ruiz de Austri, and Ki-Young Choi. Gravitino dark matter in the CMSSM and implications for leptogenesis and the LHC. *JHEP*, 08:080, 2005, hep-ph/0408227.
- [72] Christopher Savage, Graciela Gelmini, Paolo Gondolo, and Katherine Freese. Compatibility of DAMA/LIBRA dark matter detection with other searches. 2008, arXiv:0808.3607 [astro-ph].
- [73] Robert J. Scherrer and Michael S. Turner. On the Relic, Cosmic Abundance of Stable Weakly Interacting Massive Particles. *Phys. Rev.*, D33:1585, 1986.
- [74] G. Steigman. Cosmology Confronts Particle Physics. *Ann. Rev. Nucl. Part. Sci.*, 29:313–338, 1979.
- [75] Fei Wang and Jin Min Yang. SuperWIMP dark matter scenario in light of WMAP. *Eur. Phys. J.*, C38:129–133, 2004, hep-ph/0405186.
- [76] Steven Weinberg. Cosmological Constraints on the Scale of Supersymmetry Breaking. *Phys. Rev. Lett.*, 48:1303, 1982.
- [77] Ya. B. Zeldovich. *Adv. Astron. Astrophys.*, 3:241, 1965.